

Article

Fatiguing Effects on the Multi-Scale Entropy of Surface Electromyography in Children with Cerebral Palsy

Tong Hong ¹, Xu Zhang ^{1,*}, Hongjun Ma ², Yan Chen ² and Xiang Chen ¹

¹ Department of Electronic Science and Technology, University of Science and Technology of China, Hefei 230027, China; richer@mail.ustc.edu.cn (T.H.); xch@ustc.edu.cn (X.C.)

² Department of Child Rehabilitation, Jingu Hospital, Hefei 230041, China; mhj-76@163.com (H.M.); 13855124485@163.com (Y.C.)

* Correspondence: xuzhang90@ustc.edu.cn; Tel.: +86-551-6360-1175; Fax: +86-551-6360-1806

Academic Editor: Raúl Alcaraz Martínez

Received: 7 December 2015; Accepted: 18 April 2016; Published: 10 May 2016

Abstract: The objective of this study was to investigate the effects of muscle fatigue on the multi-scale entropy of surface electromyography (EMG) in children with cerebral palsy (CP) and typical development (TD). Sixteen CP children and eighteen TD children participated in experiments where they performed upper limb cyclic lifting tasks following a muscle fatiguing process, while the surface EMG signals were recorded from their upper trapezius muscles. Multi-scale entropy (MSE) analyses of the surface EMG were applied by calculating sample entropy (SampEn) on individual intrinsic mode functions (IMFs) adaptively generated by empirical mode decomposition (EMD) of the original signal. The declining degree of the resultant MSE curve was found to reflect muscle fatigue level for all subjects, with its slope (purposely calculated over the first four scales) increasing significantly as the fatigue level increased. Further, such a slope increase was less significant for CP children as compared with TD children. Our findings confirmed that the decrease of muscle fiber conduction velocity (MFCV) and the increase of motor unit synchronization may be two possible factors induced by muscle fatigue, and further indicated that there appear to be some neuromuscular changes (such as MFCV decrease, motor unit synchronization increase, motor unit firing rates reduction, selective loss of larger motor units) that occur as a result of cerebral palsy. These changes may account for experimentally observed difference in fatiguing effects between subject groups. Our study provides an investigative tool to assess muscle fatigue as well as to help reveal complex neuropathological changes underlying the motor impairments of CP children.

Keywords: cerebral palsy; electromyography; multi-scale entropy analysis; muscle fatigue

1. Introduction

Cerebral palsy (CP) is a non-progressive disorder that can induce abnormal control of posture and movement [1,2]. Activities of daily living are consequently affected by the resultant motor function deficiency. The symptoms frequently manifested for CP children include spasticity, dystonia, contractures and loss of selective motor control [3,4]. There exists various clinical methods for the assessment of neuromuscular function for CP children [5,6]. Evaluation of their ability to independently perform a specific motor task, say a sustained activity, may be one necessary approach. However, compared with their healthy peers, muscle fatigue is a more frequently reported complaint during task performance in CP children [7]. Muscle fatigue, defined as a reduction in maximal muscle force generation during sustained activity [8], is a limitation for CP children to independently accomplish a motor task. Thus for CP children, investigations into muscle fatigue may provide a way for the clinical assessment of their capacity to perform daily living activities.

Surface electromyography (EMG) measures electrical potentials during muscle activity using electrodes placed over skin surface of the muscle in a non-invasive manner. It is able to reflect the changes in motor control during muscle fatiguing contractions [9]. To quantify surface EMG signals during fatiguing processes, root mean square (RMS) of the signal amplitude [10,11], and mean power frequency (MPF) and median frequency (MDF or MF), which consider spectral distribution of the signal [12,13], are three widely used variables. An increase of signal amplitude (RMS increases) and a shift in power spectrum towards lower frequencies (MPF, MDF decreases) are expected to be indicators of muscle fatigue during isometric or isokinetic tests [10,11,13].

Various studies have shown that surface EMG signals tend to exhibit nonlinear properties [14,15]. Conventional time- or frequency-domain parameters fail to capture these properties of the surface EMG. Entropy, defined as the rate of information creation in nonlinear dynamical system, has been developed to quantitatively measure complexity of a time series signal or the system generating that signal. A variety of entropy measures, including approximate entropy (ApEn) [16], sample entropy (SampEn) [17], have been proposed as approaches to quantify complexity in nonlinear dynamical systems, with wide applications in analyses of nonstationary biomedical signals including EMG [18–21]. It has been reported in the literature [18–23] that surface EMG complexity reflects its generative processes involving recruitment and firing behaviors of active motor units during muscle contractions under regulation of the central nervous system. As illustrated in previous research [22,23], entropy of the surface EMG changes as a consequence of the increased level of muscle fatigue and serves as a better indicator of fatigue compared with traditional frequency domain parameters. Thus analyzing surface EMG using entropy measures may provide a way to evaluate fatigue and help to understand its internal mechanisms.

Moreover, it has been shown that surface EMG signals have multiple spatial and temporal scales. Multi-scale analysis of surface EMG has been reported to help characterize the structural properties of the signal, as compared with the standard single scale approach [24,25]. For example, multi-scale entropy (MSE) [26], which extends standard single-scale sample entropy to multiple time scales using “coarse-grained” approach, has shown its analytic power feasibility to assess surface EMG changes over different time scales during fatiguing muscle contraction [27]. Alternative multi-scale approaches, such as wavelet analysis [24,28] and empirical mode decomposition (EMD) [29,30], have been proposed for signal analysis. Specifically, EMD has shown its advantages in adaptively decomposing a signal into multiple representative components representing the intrinsic oscillation modes [29]. Such adaptive decomposition by EMD makes it suitable for multiscale analysis of nonstationary electrophysiological signals such as surface EMG [25]. In a recent study by Chowdhury *et al.* [31], EMD was applied to surface EMG during human walking exercise to identify muscle fatigue.

Considering how the entropy of these components changes with the increased fatigue level may provide a novel way to investigate muscle fatigue. With the above considerations, in the current study, a novel MSE analysis was applied to surface EMG from children with CP or typical development (TD) for examining muscle fatigue during upper limb lifting tasks. The MSE method used in this study computes SampEn over different time scales represented by intrinsic mode functions (IMFs) derived from EMD decomposition of an original surface EMG time series. The findings of this study demonstrated that the MSE of surface EMG can serve as an appropriate indicator of muscle fatigue. Moreover, investigation into MSE changes of surface EMG during fatiguing muscle contractions can help better understand regulation mechanisms of the central nervous system and neuropathological mechanisms underlying motor impairments of CP.

2. Method

2.1. Subjects

Sixteen children diagnosed with CP (12 males, four females, age: 7.4 ± 2.3 years, mean \pm standard deviation) were recruited in our research. For comparison, eighteen age-matched healthy children

with typical development (TD) (11 males, seven females, age: 7.9 ± 1.6 years) without any known neurological deficiencies also participated in our study as the control group. All CP participants were recruited from Jingu Hospital (Hefei, China) which is devoted to the treatment and rehabilitation of CP children. All TD children were recruited from faculty family at the University of Science and Technology of China (USTC, Hefei, China). The study with recruitment of human subjects was approved by ethic review boards of both institutes. The inclusion criteria of CP children participating in our research include: (1) age between 4 and 13 years old; (2) no abnormal postures or involuntary movements were shown during upper limb lifting task performance; (3) ability to independently complete tasks without some external assistance; (4) ability to sustain some extent of external loads; (5) ability to comprehend instructions from researchers; (6) no history of other kinds of pathological cause that lead to the motor function deficiency despite cerebral palsy. For each CP child, upper limb function was evaluated by manual ability classification system (MACS) proposed by Eliassen *et al.* [32], which classifies CP children's manual ability by observing how they use their upper limbs to handle objects in daily activities. The information of all CP children was shown in Table 1.

Table 1. Information of all CP children.

Subject	Gender	Age (Years)	Diagnosis	MACS	Tested Limb	MLF (N)
CP1	M	7.2	Spastic	II	R	35
CP2	M	5.0	Spastic	II	R	28
CP3	M	8.4	Spastic	I	L	53
CP4	M	5.0	Spastic	II	R	30
CP5	M	4.5	Spastic	II	R	18
CP6	F	7.0	Spastic	I	R	54
CP7	F	4.8	Spastic	II	R	20
CP8	F	12.2	Spastic	II	R	36
CP9	M	8.3	Spastic	I	R	43
CP10	M	5.7	Spastic	III	L	16
CP11	M	11.7	Right hemiplegia	I	R	57
CP12	M	8.3	Right hemiplegia	II	R	40
CP13	F	6.5	Right hemiplegia	II	R	24
CP14	M	7.0	Right hemiplegia	III	R	22
CP15	M	9.6	Right hemiplegia	II	R	47
CP16	M	6.7	Right hemiplegia	II	R	35

In addition, none of the recruited TD children had any neuromuscular problems in their upper limbs and their information is shown in Table 2. Written consent was obtained from the guardians of all CP and TD children prior to their participation in the study.

Table 2. Information of all TD children.

Subject	Gender	Age (Years)	Tested Limb	MLF (N)
TD1	M	7.8	R	36
TD2	M	8.3	R	53
TD3	M	7.0	R	60
TD4	M	6.7	R	45
TD5	M	5.2	R	28
TD6	F	11.0	R	60
TD7	F	7.3	R	40
TD8	M	7.0	R	35
TD9	M	7.0	R	60
TD10	F	7.4	R	38
TD11	M	12.3	L	68
TD12	M	8.0	R	62
TD13	F	8.3	R	44
TD14	F	7.4	R	42
TD15	F	8.7	R	60
TD16	F	8.5	L	53
TD17	M	7.7	L	46
TD18	M	7.0	R	57

2.2. Experiment

In our experiments, participants were required to continuously lift their tested limb up and down within a fixed vertical distance until they were unable to sustain the performance due to the fatigue of the associated muscle. The vertical distance, which was equally divided by the equilibrium position, was determined prior to task performance. The equilibrium position was defined as the position where the shoulder was flexed to 90 degrees and the upper limb was stretched forward, parallel to the ground, with a full extension in the elbow. Since the length of the limb for each subject was a fixed quantity and measured as l , the angle α between the equilibrium position and the top/bottom lifting position was used to determine the vertical distance $s = 2l\sin\alpha$, as illustrated in the Figure 1a.

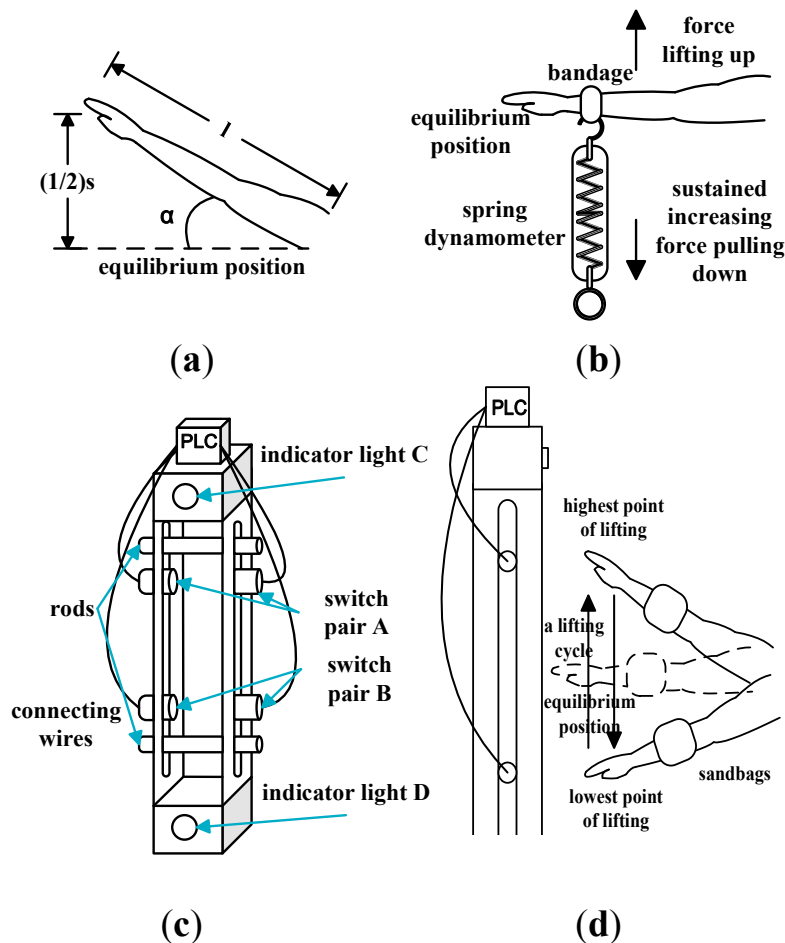


Figure 1. (a) Illustration of vertical distance determination; (b) Illustration of MLF determination; (c) The apparatus; (d) Upper limb lifting with sandbags tied on the limb. Arrows denoted a lifting cycle.

The maximum lifting angle was set as $\alpha = 30^\circ$ for both TD and cerebral palsy subjects. It was verified that all CP children recruited in our experiment could lift their limb over that vertical distance without any external assistance.

A load determination was performed for each subject before the experiment. The maximum lifting force (MLF) for each subject, was measured as the maximum level of force that the subject was able to exert in order to maintain the tested limb at the equilibrium position against a sustained increasing force along the gravitational direction. Each subject was first asked to unbend the tested limb and maintain it at the equilibrium position. Then a soft inelastic bandage was tied on the wrist. A spring dynamometer with maximum measurement capacity 100 N was used by researchers to measure force, the hanging hook of which was fixed tightly on the bandage. During the whole measurement

process, as illustrated in Figure 1b, researchers pulled the dynamometer downward vertically with a sustained increasing force and subjects were required to try their best to maintain their limb at the equilibrium position. However, at the instance when the limb was pulled down about 10° deviating from the equilibrium position, the force recorded by the dynamometer was regarded as the MLF. In order to get reliable and accurate results, the measurement was repeated twice for each subject. The interval between two successive measurements was about 5 min. The higher value between both measurements was regarded as the final MLF value for each participant. MLF values for all the CP children (35 ± 13 N) and all the TD subjects (49 ± 11 N) are shown in Tables 1 and 2 respectively. After the MLF was obtained for each subject, three different loads, expressed as 0%, 30% and 60% of the MLF, were calculated. These external loads were represented by weight-adjustable sandbags which were tied tightly on the tested limb during task performance. Each subject was asked to perform three different fatiguing tasks, each with a predefined load, respectively. The load presentation was randomized in our experiments.

In order to perform the muscle fatigue protocol in a more sensible and controllable way, we devised a convenient apparatus using some affordable electronic devices. As shown in Figure 1c, the main part of the apparatus was a cuboid-like rigid frame of which the height was fixed at 1500 mm. The inside of the apparatus was empty to allow the upper limb of participants lifting inside. There were two long slots opened on it, one on the left side and the other on the right side. Two pairs of infrared radiation switches (24 V DC), called switch pair A and switch pair B, could be moved and placed at arbitrary positions on the slots using screw bolts. After determining the equilibrium position for each subject, the switch pair A and B were placed on the slots about half of the lifting vertical distance above and below the equilibrium position, respectively. Additional pair of long rods were placed about 1 to 2 cm apart from the switch pair A and B, in order to limit the vertical range for the subject to perform the arm lifting task. The output states of these two switch pairs (A and B) were recorded by a programmable logic controller (PLC, S7-2006ES7222-1BB23-0XB8, Siemens, Munich, Germany) installed on the top of the apparatus, and were used to control two indicator lights C and D, respectively. When the tested arm passed through a switch pair (A for example), it was turned off and its corresponding light indicator (C for example) was turned on. Thus whether the designed position can be reached or not could be ascertained by observing the states of two indicator lights when the arm was swing up and down inside the empty part of the apparatus (Figure 1d).

Before task performance, subjects were instructed to remain fully relaxed without any physical activity for at least two hours. After familiarization with the apparatus and experimental process, subjects were positioned in a height-adjustable chair. Each task with a predefined load consisted of two trials. The interval between any two successive tasks and two trials was sufficiently long to allow the fatigued muscles to fully recover. During task performance, subjects sit in front of the apparatus and their tested limb was lifted inside of the apparatus with a fixed vertical distance determined by positions of two switch pairs (Figure 1d). The beginning position of the arm was the lowest points of the vertical distance (namely, the position of switch pair B) and a lifting cycle was made when the arm was lifted to the highest point (the position of switch pair A) and returned back to the lowest point of the entire vertical distance. Subjects were asked to try their best to reach the highest point in each cycle. During fatiguing protocol, it became difficult for subjects to reach the determined vertical distance as a result of increased level of muscle fatigue. We assumed full fatigue of the related muscles if the highest point could not be reached for four successive cycles, and then the task performance was terminated. Oral encourages were essential for every subject during each trial.

Surface EMG was recorded using a home-made data recording system from the upper trapezius muscle, which was regarded to be highly involved in upper limb lifting. The surface EMG sensor used in this study consisted of two parallel bar-shaped electrodes in a size of 1 mm \times 10 mm with an electrode-to-electrode distance of 10 mm to constitute a signal-differential recording channel. These two electrodes were placed on the skin surface in the middle of the tested upper trapezius muscle along the muscle fibers. The surface EMG signals were band-pass filtered between 20 Hz and 500 Hz and

were further sampled at 1 kHz. All recorded surface EMG data was stored to the hard disk of a laptop computer for further analysis using Matlab (Version 2013, The Mathworks Inc., Natick, MA, USA).

2.3. Data Segmentation

From visual inspection of the recorded data, a surface EMG time series during each trial showed a series of muscle activity bursts, each corresponding to a muscle contraction during the upper limb lifting up (see Figure 2). For each trial, a segment of surface EMG data between the onset of the first muscle activity burst and offset of the last one was selected. The signal within the last four cycles of upper limb lifting were further discarded since the task performance in that period may not meet the basic requirement as a result of muscle fatigue. The remaining surface EMG segment was further divided into three non-overlapping data windows of equal duration (see Figure 2a). The resultant three data windows were denoted as W1, W2 and W3, being the first, second and final thirds of the surface EMG segment recorded in each trial, to account for three different levels of muscle fatigue. Then the following MSE analysis was performed on each data window.

2.4. MSE Analysis

2.4.1. Empirical Mode Decomposition

Empirical mode decomposition (EMD) method, proposed by Huang *et al.* [29], is a time-frequency analysis method for adaptive decomposition of a signal into a set of intrinsic mode functions (IMFs) representing its intrinsic oscillation modes in the signal. Due to its advantages, EMD has been successfully used in the analysis of non-linear and non-stationary biomedical signals including EMG [31,33,34]. These resultant IMFs can also be considered as different scales of the original signal for multi-scale analysis [25]. The EMD process requires that upper and lower envelopes defined by identifying local extremes of the original signal $s(t)$ should be created first. The upper envelope is created by cubic spline interpolation between local maximums. Analogously, the lower envelope is derived from local minimums. Then, the mean of two envelopes is calculated as $m(t)$ and is subtracted from $s(t)$.

The residual signal $d(t)$ is regarded as an IMF if it satisfies two conditions. The first condition is that the number of all local extremes (including maximums and minimums) is equal to the number of zero-crossings of the signal or their difference is one. The second is that the mean of two envelopes of the signal is zero. However, if the above two conditions are not satisfied, the signal $d(t)$ cannot be regarded as an IMF. Under this circumstance, the mean of its two envelopes is subtracted and the process described above is repeated on the residual signal until a true IMF is identified. After an IMF is extracted from the original signal $s(t)$, the above analysis is iterated on the residue to further get other IMFs. Such iteration is referred to as the sifting process. The whole process terminates when the final residue is a monotonic function or a function with only one extreme. Overall, the sums of all IMFs extracted approximately equal to the original signal:

$$s(t) = \sum_{i=1}^n IMF_i + r_n \quad (1)$$

where n is the total number of IMFs extracted, r_n is the final residue.

2.4.2. Sample Entropy

Sample entropy (SampEn), originally proposed by Richman and Moorman [17], is an effective measure of the complexity of short time series, with wide applications in analyzing non-linear and non-stationary biomedical signals including EMG [21,35,36].

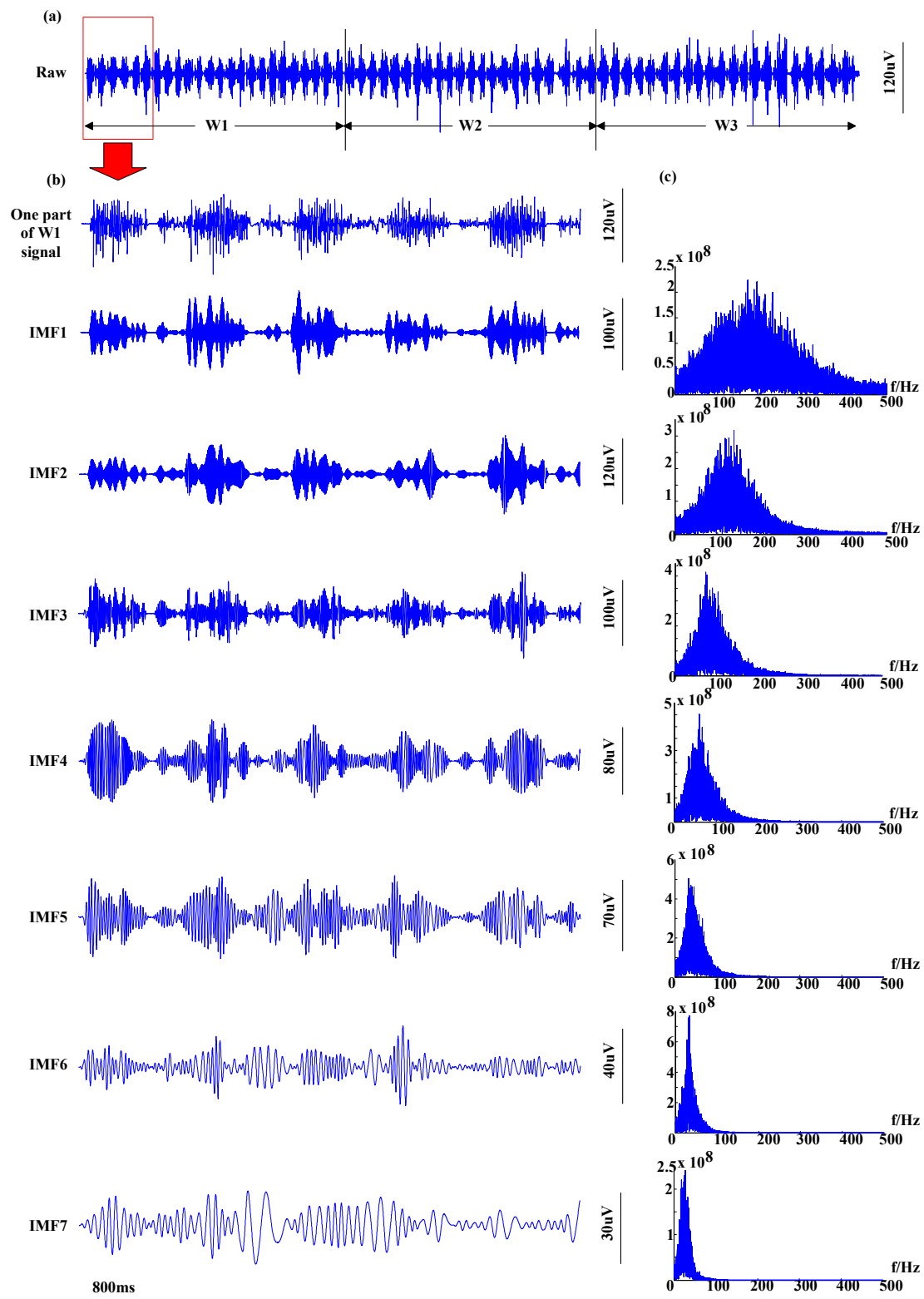


Figure 2. Decomposition results of a representative surface EMG signal from one TD subject (TD2) under 0% load. (a) Raw sEMG signal segmented by three windows with an equal length; (b) One part selected from the W1 signal in detail and its corresponding 7 IMFs after EMD; (c) The power spectra of corresponding IMFs.

To calculate the sample entropy of a scalar time series $\{x_1, x_2, \dots, x_N\}$ with length N , the first step is to embed this time series in a delayed m -dimensional space, where vectors are defined as:

$$X_m(i) = [x(i), x(i+1), \dots, x(i+m-1)] \quad (i = 1, 2, \dots, N-m) \quad (2)$$

Then for each $X_m(i)$, the number of all other vectors which satisfy the condition that their distances from $X_m(i)$ are smaller than the tolerance r is counted as $N(i)$. Next the frequency of occurrence $B_i^m(r)$ is calculated as $N(i)/(N-m-1)$, and $B_i^m(r)$ is averaged over all i :

$$B^m(r) = \frac{1}{N-m} \sum_{i=1}^{N-m} B_i^m(r) \quad (3)$$

By increasing the dimension to $m+1$, we can similarly get $B^{m+1}(r)$ using process described above. Finally, the sample entropy is calculated as:

$$\text{SampEn}(m, r, N) = -\ln\left(B^{m+1}(r)/B^m(r)\right) \quad (4)$$

The dimension m and the tolerance r need to be determined before entropy calculation. With reference to the literature [17,26,37], the tolerance r can be selected as between $0.15 \times \text{SD}$ and $0.25 \times \text{SD}$, where SD is the standard deviation of the input time series. The use of larger tolerance was also recommended for relatively shorter time series [17]. Based on some pretests, the parameters were selected as $m = 2$, $r = 0.2 \times \text{SD}$ in our study.

2.4.3. EMD-Enhanced MSE Analysis

With EMD acting as a multi-scale analysis tool to decompose input data (each data window in this study) into IMFs, the MSE can be straightforwardly performed by applying SampEn on each resultant IMF. The MSE analysis was performed independently on each data window to produce a series of SampEn values, forming a MSE curve over multiple scales (*i.e.*, IMFs). The mean of the MSE curves derived from two trials of the same task (with the same load) was calculated for each subject. For each of three different loads, the MSE curves were further averaged over all subjects in each subject group, for the comparison between the CP group and the control group.

2.5. Statistical Analysis

It was found in our study that the EMD produced 7 IMFs for all surface EMG data windows (see Figure 2), and that the subsequent MSE curves showed an evident declining trend across all trials and all subjects as the IMF order increased (see Figure 3). In order to assess the fatiguing effect on the MSE results, a linear regression analysis was performed on SampEn values at the first four IMF orders (*i.e.*, IMF1-4), and the slope was obtained to represent the declining degree of the MSE curve for each data window.

The reason for using first four IMF orders to account for the fatiguing effect was a significant change in their entropy declining trend with increasing level of muscle fatigue (from W1 to W3), as explained in the following experimental results.

In order to examine the effect of fatigue (represented by the data windows) and the load on the MSE results, and to identify difference of such effect between two subject groups, a mixed linear model was applied on the slope values, with the window (three levels: W1, W2 and W3) and the load (3 levels: 0%, 30% and 60%) considered as both within-subject factors and the group (2 levels: CP *vs.* TD) considered as the between-subject factor. A series of post-hoc pairwise multiple comparisons with Bonferroni correction were used. The level of statistical significance was set as $p < 0.05$ for all analyses. All statistical analyses (including linear regression) were carried out using SPSS software (Version 16.0, SPSS Inc., Chicago, IL, USA).

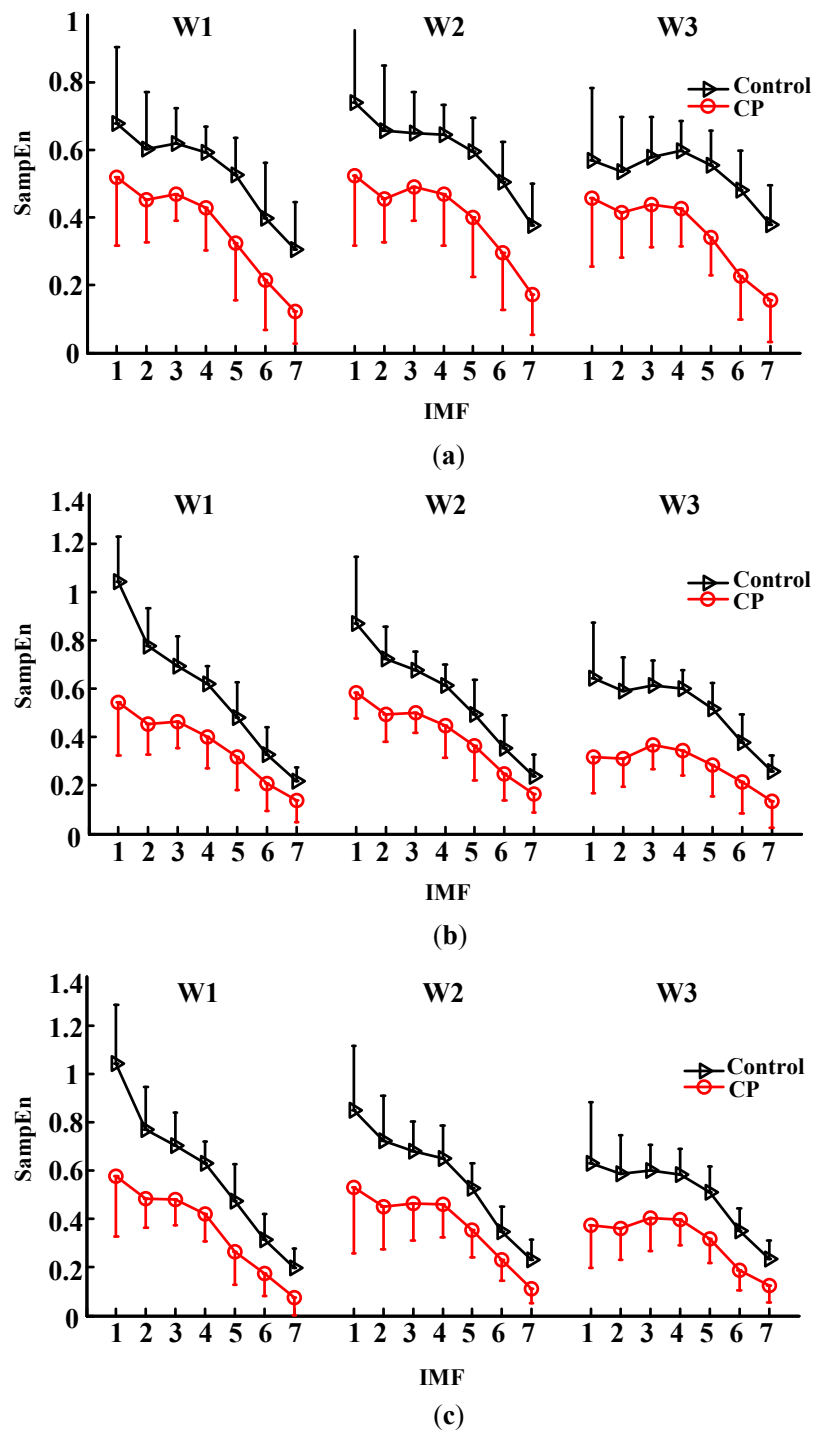


Figure 3. MSE curves averaged across subjects in each of the control group and the CP group under three fatigue degrees (windows) and three loads: (a) 0% load; (b) 30% load; (c) 60% load, respectively.

3. Results

For both two subject groups and all three loads, the total number of IMFs extracted was seven for each signal window. The results of data segmentation and decomposition for one TD subject (TD2) were used as an example and shown in Figure 2. In Figure 2a, the raw EMG signal segment under 0% load was divided by three signal windows of equal length: W1, W2 and W3. The 7 IMFs derived from the signal window W1 via EMD were shown in Figure 2b in details. In addition, power spectrum of each corresponding IMF was also shown in Figure 2c, thus confirming that higher-order IMFs tended

to carry relatively lower-frequency components (representing longer-term temporal scales) of the original signals.

For both two groups, the mean MSE curves averaged over all subjects in each of CP and TD groups under three different loads were shown in Figure 3, with the error bars indicated the standard deviations. It can be observed from Figure 3 that for both two subject groups, the MSE curves showed an evident declining trend with the increase of IMF order. Furthermore, the visually observed declining degree of MSE curve varied across three data windows. This was especially the case for the SampEn values at the beginning four IMF orders (namely, IMF1 to IMF4). For TD subjects under load 0% (Figure 3a), an obvious entropy declining trend could be seen from the signal window W1 which represented the lowest level of muscle fatigue. For the window W2, the entropy value of IMF4 was almost in the same level with IMF2 and IMF3. In window W3, compared with IMF1, entropy of IMF3 and IMF4 relatively increased, thus leading to an even locally increasing trend from IMF1 to IMF4. Consequently, the degree of entropy declining was found to reduce from window W1 to W3. Consistent trend was also found under other two loads for the control group and all three loads for the CP group. In addition, the load was also observed to be a factor that affected the decline of the MSE curve. For each group under load 30% (Figure 3b), compared with load 0% (Figure 3a), entropy values of IMF3 and IMF4 in window W3 were at the same level as or even climbed beyond those at IMF1. By contrast, for both two subject groups, the declining trend remained the same at higher IMF orders (namely, IMF5 to IMF7), regardless of the load or the fatigue degree (data windows).

In order to characterize the experimentally observed fatiguing effect on the MSE curve, a linear regression was performed on the SampEn values at the first four IMF orders, for each data window from a subject. The resultant mean slope values, averaged across subjects in each group, was shown in Figure 4 for three signal windows and three loads, respectively, where the error bars indicated the standard deviations. It was found that the mean slope value for both two groups increased from window W1 to W3.

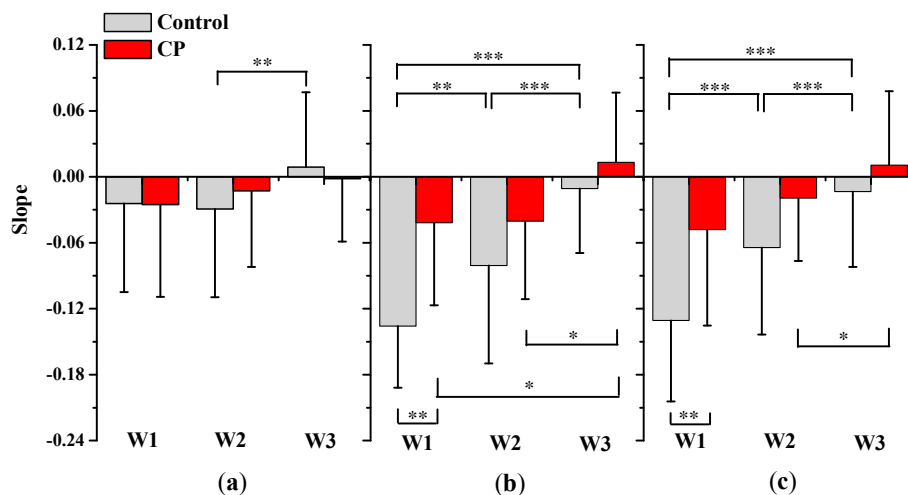


Figure 4. Mean slope values averaged across subjects in each of two groups for three fatigue degrees (W1, W2 and W3) and three loads: (a) 0% load; (b) 30% load; (c) 60% load, respectively. Asterisks indicate statistical significance in multiple pairwise comparisons: * $0.01 < p < 0.05$; ** $0.001 < p < 0.01$; *** $p < 0.001$.

The mixed linear model reported an overall significant effect of all the window ($F = 85.944$, $p < 0.001$), the load ($F = 5.17$, $p = 0.02$) and the group ($F = 6.143$, $p = 0.019$) on slope values. Moreover, a significant interaction between any two ($p < 0.041$) or among all three factors ($F = 2.885$, $p = 0.035$) was revealed as well. Significant slope increase was reported for the control group when the fatigue level increased from W1 to W3, while no significant difference between windows was found for the CP

group. Under 0% load, the window W3 yielded higher slope value than W2 with statistical significance ($p = 0.007$) for the control group, while no significant difference was revealed between any two of three signal windows ($p = 1$) for the CP group. Under 30% load, significant difference was observed between every two windows of control group ($p < 0.003$), while a significant difference was only seen between W1 and W3 ($p = 0.016$), and between W2 and W3 ($p = 0.019$) for the CP group. Under 60% load, a significant difference was observed for every two windows ($p < 0.001$) for the control group, while a significant difference was only found between W2 and W3 ($p = 0.014$) for the CP group.

Statistical analysis revealed that load had significant effect on slope values for the control group, whereas such effect was not significant for the CP group. For window W1, a significant difference was seen between 0% load and any of the other two loads ($p < 0.001$) for the control group. However, there was no difference between 30% load and 60% load ($p = 1$). For window W2, a significant difference was revealed between 0% load and 30% load ($p = 0.029$), while no difference was revealed for any other comparisons ($p > 0.05$). For window W3, no difference was revealed between any two loads, with $p > 0.05$ for every two loads. For each signal window of the CP group, $p = 1$ was found for comparisons between every two loads.

When considering difference in MSE slope between two groups, statistical significance was reported for W1 under load 30% ($p = 0.003$) or 60% ($p = 0.005$), while no significance was found for any other windows under any other loads ($p > 0.05$).

4. Discussion

Empirical mode decomposition can adaptively decompose a complicated time series into a finite number of intrinsic mode functions (IMFs) [29]. Compared with the “coarse-grained” approach [26] and the wavelet analysis [24,28], EMD uses a so-called sifting process which is adaptive and makes no assumption about the original signal. The proposed EMD-driven MSE analysis was performed to apply entropy estimate to individual IMFs which represent the intrinsic oscillation modes of the original signal. In our study, we investigated how the MSE of surface EMG changes with the increased level of muscle fatigue in children with TD and CP.

By calculating SampEn values over multiple IMFs of surface EMG, the resultant MSE curve showed a general trend of direct decline with increasing IMF orders. The reason for explaining the declining trend of MSE curve can be the sifting process involved in the EMD algorithm. Since the number of extrema decreases during residue iterations in the sifting process, the corresponding spectral quantities can accordingly decrease [38]. As a result, higher order IMFs tend to become more regular by carrying more slowly oscillatory modes (as demonstrated by the spectral analysis of IMFs in Figure 2) in the original signals, consequently yielding smaller SampEn values. This was found to be evident without significant muscle fatigue (for W1). Moreover, our study further revealed that the declining trend of MSE was expected to decrease or even to change to an increasing trend as a result of increased fatigue level (from W1 to W3), regardless of any subject group. Specifically, such change in MSE curve was visually observed to be evident at the first four IMF orders. Therefore, the slope from a linear regression of SampEn values at first four IMF orders was proposed to quantify the fatiguing effect on MSE curve. On this basis, the increase in slope values was found from W1 to W3, with overall statistical significance revealed by the mixed linear model. The decreased declining trend of MSE (*i.e.*, increased slope) reflected a relative increase in entropy of lower oscillation modes (higher IMF orders) during the fatiguing process (from W1 to W3).

Muscle fatigue is a complex physiological process that involves interactions of multiple neuro-muscular variables [8,9]. Our MSE analysis suggested a relative increase in entropy values of lower oscillation modes with respect to those of higher oscillation modes as a result of muscle fatigue. This may be the consequence of the decrease in muscle fiber conduction velocity (MFCV) [8,9,39,40] during the muscle fatiguing process. It has been widely recognized that the recorded EMG signal is composed of several motor unit action potentials (MUAPs) which reflect the electrical activity of anatomical motor units [27,41]. At the single motor unit level, decrease in fiber conduction velocity

may lead to the reduction in the sharpness of the discharged MUAP, resulting in much smoother and wider MUAP waveform. Therefore, from the whole EMG signal's perspective, decrease in MFCV may lead to slow oscillations of the signal, thus increasing the portion of lower oscillation modes carried in the original signal. This change in signal structure might lead to the increase in entropy of corresponding higher order IMFs, thus decreasing the declining trend in MSE curve. Another reason for explaining the relative increase of entropy values at the third and fourth IMF orders may be the increased motor unit synchronization, which has been reported as a possible factor contributing to surface EMG alternations as a result of fatigue [8,9,27,42,43]. Synchronization is defined as the almost simultaneous discharge of MUAPs in motor units. Therefore, the resultant overlapped MUAP may tend to show a smoother and enlarged waveform with a broadened time course, thereby having lower oscillation modes in the resultant surface EMG recording. Similarly, an increase in motor unit synchronization as a result of muscle fatigue may also contribute to a relative increase in entropy of higher order IMFs (decrease in entropy declining trend). Our findings based on MSE analysis showed some accordance with previous reports relying on spectral analysis for muscle fatigue assessment. It has been widely recognized that surface EMG spectral parameters, such as mean power frequency (MPF) and median frequency (MDF), showed a declining trend during fatiguing process [12,13,44,45], which confirmed power spectrum shift toward lower-frequency bands [39,40,46–48]. Considering the nature of the sifting process of EMD that higher order IMFs represent lower frequency components in the original EMG signals, power spectrum's shifting toward lower-frequency bands may lead to the increase in the proportions of lower frequency components (higher order IMFs) in the original signals. Consequently, entropy values of higher order IMFs are relatively increased, leading to a decrease in entropy declining trend.

Although alterations in slope of MSE curve at the beginning four IMF orders could be observed as a result of muscle fatigue for both subject groups, such a slope increase found from W1 to W3 in the CP group was not as statistically significant as that in control group. This different fatigue induced consequence assessed by the MSE between two groups may reflect complex neural or muscular changes at work underlying the motor impairment of CP. Specifically, the above-mentioned muscle fatigue-related changes, including MFCV decrease and motor unit synchronization increase, may have been already involved in muscles of CP children. On one hand, predominance of type I muscle fibers and atrophy of type II fibers have been reported to take place in muscles of CP patients [49–52]. This morphological and structural changes in muscles may be the consequence of the selective loss of larger motor units (with higher MFCV) [53]. As a result, relatively smaller and lower-threshold motor units are very likely to be recruited for CP children during their voluntary muscle contractions, primarily with type I fibers which are less fatigable than type II fibers. Consequently, the reduction in overall conduction velocity of muscle fibers during fatiguing process was not significant for CP patients as compared with TD children. On the other hand, higher level of synchronization and broader duration of synchronization may be the resulted from lesions of the central nervous system and have been reported in subjects with neurological disorders or injuries such as stroke, spinal cord injury, or CP [54,55]. Thus, such synchronization degree may not change much for CP during fatiguing muscle contractions. When the increase in slope of MSE curve was considered as an indicator of muscle fatigue, less change in this indicator for CP patients exhibited their impaired capability of motor control regulation adaptive to fatiguing muscle contraction.

Besides, load acted as a factor that affected MSE results as well. It was found from the Figure 2 that higher load percentages tended to yield higher MSE values especially at lower order IMFs. Moreover, the MSE curves derived from the TD group lay beyond those from the CP group, regardless of any window or any load. This is primarily due to relatively lower muscle contraction intensity in the CP group given the same load percentage, as a result of their insufficient ability of force production.

It has been recognized that the number of active motor units and their firing rates are two factors which modulate the force generation during muscle contraction [53,56].

Thus for higher level of muscle contraction, more motor units are recruited and their overall firing rates are increased. As a result, for TD subjects, MSE values in each signal window increased from 0% load to 60% load. This was specifically evident at lower-order IMFs, since the higher oscillation modes tended to show higher increases in entropy values. For each signal window, the discrepancy between entropy values of higher and lower oscillation modes became larger and a more significant declining entropy trend could be seen when the load was increased from 0% to 60%, as showed in Figure 3. However, this was not true for CP patients. Statistical analysis revealed that loads had no significant effect on their entropy declining trend. As it has been described above that CP patients may have limited capability to increase motor unit firing rates, the only way for higher force production under some extent of external loads was just to recruit more additional motor units. In this regard, some larger and higher threshold motor units are likely to be recruited even at relatively lower force level. Further, due to selective loss of larger motor units, the number of all motor units to be recruited in muscles of CP patients may be limited as well. As a result, they truly showed limited capability of force production, which inhibited the increase in MSE values when loads quantity increases.

In order to fully reveal the motor control mechanisms underlying changes in the declining entropy trend during fatiguing muscle contractions of CP children, more diagnostic indicators and investigative tools need to be incorporated, due to their lesions of the central nervous system and impaired motor pathways. In addition, our study showed statistically significant differences in entropy declining trend between TD and CP subjects at the group level. However, significant differences between individual subjects were not demonstrated. A larger study with many more CP participants to assess differences at the individual subject level is needed for the possible application of our method to clinical diagnosis.

5. Conclusions

Our study examined entropy of all IMFs obtained by EMD in surface EMG signals during fatiguing process in children with CP and TD. We discovered that the declining trend of the MSE curves decreased during muscle fatiguing process. This finding can be attributed to a MFCV decrease and motor unit synchronization increase in fatiguing muscles. Compared with a significant increase in slope of MSE curve with the increased muscle fatigue level for TD subjects, such a slope increase was not significantly observed for CP children. There appears to be complex neuromuscular changes (such as MFCV decrease, motor unit synchronization increase, motor unit firing rates reduction, selective loss of larger motor units) occurring as a result of cerebral palsy that may account for the experimentally observed differences between subject groups. Our study may provide a new way to assess muscle fatigue as well as to help reveal the complex neuropathological changes underlying the typical motor impairments of CP children.

Acknowledgments: The authors thank Ruixing He and Lu Tang for their help with data collection. This work was supported in part by the Fundamental Research Funds for the Central Universities of China (Grants #WK2100230014) and the National Nature Science Foundation of China (NSFC) (Grants # 61271138).

Author Contributions: Tong Hong designed the research, took part in the experiments, processed and analyzed the data, interpreted the results, and drafted the paper. Xu Zhang analyzed the data, interpreted the results, and performed critical revision of the paper. Hongjun Ma took part in the experiments and interpreted the results. Yan Chen interpreted the results. Xiang Chen conceived the study and interpreted the results. All authors have read and approved the final manuscript.

Conflicts of Interest: The authors declare no conflict of interest.

References

1. Bax, M.; Goldstein, M.; Rosenbaum, P.; Leviton, A.; Paneth, N.; Dan, B.; Jacobsson, B.; Damiano, D. Proposed definition and classification of cerebral palsy, April 2005. *Dev. Med. Child Neurol.* **2005**, *47*, 571–576. [[CrossRef](#)] [[PubMed](#)]
2. Rosenbaum, P.; Paneth, N.; Leviton, A.; Goldstein, M.; Bax, M.; Damiano, D.; Dan, B.; Jacobsson, B. A report: The definition and classification of cerebral palsy April 2006. *Dev. Med. Child Neurol. Suppl.* **2007**, *109*, 8–14. [[PubMed](#)]

3. Gormley, M.E., Jr. Treatment of neuromuscular and musculoskeletal problems in cerebral palsy. *Dev. Neurorehabil.* **2001**, *4*, 5–16.
4. Morris, C. Definition and classification of cerebral palsy: A historical perspective. *Dev. Med. Child Neurol.* **2007**, *49*, 3–7. [[CrossRef](#)]
5. Ketelaar, M.; Vermeer, A.; Helders, P.J. Functional motor abilities of children with cerebral palsy: A systematic literature review of assessment measures. *Clin. Rehabil.* **1998**, *12*, 369–380. [[CrossRef](#)] [[PubMed](#)]
6. Scholtes, V.A.; Becher, J.G.; Beelen, A.; Lankhorst, G.J. Clinical assessment of spasticity in children with cerebral palsy: A critical review of available instruments. *Dev. Med. Child Neurol.* **2006**, *48*, 64–73. [[CrossRef](#)] [[PubMed](#)]
7. Jahnsen, R.; Villien, L.; Stanghelle, J.K.; Holm, I. Fatigue in adults with cerebral palsy in Norway compared with the general population. *Dev. Med. Child Neurol.* **2003**, *45*, 296–303. [[CrossRef](#)] [[PubMed](#)]
8. Gandevia, S. Spinal and supraspinal factors in human muscle fatigue. *Physiol. Rev.* **2001**, *81*, 1725–1789. [[PubMed](#)]
9. De Luca, C.J. Myoelectrical manifestations of localized muscular fatigue in humans. *Crit. Rev. Biomed. Eng.* **1983**, *11*, 251–279.
10. Crenshaw, A.; Karlsson, S.; Gerdle, B.; Friden, J. Differential responses in intramuscular pressure and EMG fatigue indicators during low-*vs.* high-level isometric contractions to fatigue. *Acta Physiol. Scand.* **1997**, *160*, 353–361. [[CrossRef](#)] [[PubMed](#)]
11. Croce, R.; Miller, J. Angle-and velocity-specific alterations in torque and semg activity of the quadriceps and hamstrings during isokinetic extension-flexion movements. *Electromyogr. Clin. Neurophysiol.* **2005**, *46*, 83–100.
12. Komi, P.V.; Tesch, P. EMG frequency spectrum, muscle structure, and fatigue during dynamic contractions in man. *Eur. J. Appl. Physiol. Occup. Physiol.* **1979**, *42*, 41–50. [[CrossRef](#)] [[PubMed](#)]
13. Yamada, H.; Kaneko, K.; Masuda, T. Effects of voluntary activation on neuromuscular endurance analyzed by surface electromyography. *Percept. Motor Skills* **2002**, *95*, 613–619. [[CrossRef](#)] [[PubMed](#)]
14. Lei, M.; Wang, Z.; Feng, Z. Detecting nonlinearity of action surface EMG signal. *Phys. Lett. A* **2001**, *290*, 297–303. [[CrossRef](#)]
15. Rodrick, D.; Karwowski, W. Nonlinear dynamical behavior of surface electromyographical signals of biceps muscle under two simulated static work postures. *Nonlinear Dyn. Psychol. Life Sci.* **2006**, *10*, 21–35.
16. Pincus, S.M. Approximate entropy as a measure of system complexity. *Proc. Natl. Acad. Sci. USA* **1991**, *88*, 2297–2301. [[CrossRef](#)] [[PubMed](#)]
17. Richman, J.S.; Moorman, J.R. Physiological time-series analysis using approximate entropy and sample entropy. *Am. J. Physiol. Heart Circ. Physiol.* **2000**, *278*, H2039–H2049. [[PubMed](#)]
18. Abásolo, D.; Hornero, R.; Espino, P.; Poza, J.; Sánchez, C.I.; De La Rosa, R. Analysis of regularity in the EEG background activity of Alzheimer’s disease patients with Approximate Entropy. *Clin. Neurophysiol.* **2005**, *116*, 1826–1834. [[CrossRef](#)] [[PubMed](#)]
19. Ahmad, S.A.; Chappell, P.H. Moving approximate entropy applied to surface electromyographic signals. *Biomed. Signal Process. Control* **2008**, *3*, 88–93. [[CrossRef](#)]
20. Chen, W.-T.; Wang, Z.-Z.; Ren, X.-M. Characterization of surface EMG signals using improved approximate entropy. *J. Zhejiang Univ. Sci. B* **2006**, *7*, 844–848. [[CrossRef](#)] [[PubMed](#)]
21. Zhang, X.; Zhou, P. Sample entropy analysis of surface EMG for improved muscle activity onset detection against spurious background spikes. *J. Electromyogr. Kinesiol.* **2012**, *22*, 901–907. [[CrossRef](#)] [[PubMed](#)]
22. Lee, T.-R.; Kim, Y.H.; Sung, P.S. Spectral and entropy changes for back muscle fatigability following spinal stabilization exercises. *J. Rehabil. Res. Dev.* **2010**, *47*, 133–142. [[CrossRef](#)] [[PubMed](#)]
23. Sung, P.S.; Zurcher, U.; Kaufman, M. Comparison of spectral and entropic measures for surface electromyography time series: A pilot study. *J. Rehabil. Res. Dev.* **2007**, *44*, 599. [[CrossRef](#)] [[PubMed](#)]
24. Kaplanis, P.A.; Pattichis, C.S.; Zazula, D. Multiscale entropy-based approach to automated surface EMG classification of neuromuscular disorders. *Med. Biol. Eng. Comput.* **2010**, *48*, 773–781.
25. Zhang, X.; Chen, X.; Barkhaus, P.E.; Zhou, P. Multiscale entropy analysis of different spontaneous motor unit discharge patterns. *IEEE J. Biomed. Health Inform.* **2013**, *17*, 470–476. [[CrossRef](#)] [[PubMed](#)]
26. Costa, M.; Goldberger, A.L.; Peng, C.-K. Multiscale entropy analysis of complex physiologic time series. *Phys. Rev. Lett.* **2002**, *89*, 068102. [[CrossRef](#)] [[PubMed](#)]

27. Cashaback, J.G.; Cluff, T.; Potvin, J.R. Muscle fatigue and contraction intensity modulates the complexity of surface electromyography. *J. Electromyogr. Kinesiol.* **2013**, *23*, 78–83. [[CrossRef](#)] [[PubMed](#)]
28. Mallat, S.G. A theory for multiresolution signal decomposition: The wavelet representation. *IEEE Trans. Pattern Anal. Mach. Intell.* **1989**, *11*, 674–693. [[CrossRef](#)]
29. Huang, N.E.; Shen, Z.; Long, S.R.; Wu, M.C.; Shih, H.H.; Zheng, Q.; Yen, N.-C.; Tung, C.C.; Liu, H.H. The Empirical Mode Decomposition and the Hilbert Spectrum for Nonlinear and Non-Stationary Time Series Analysis. *Proc. R. Soc. Lond. A Math. Phys. Eng. Sci.* **1998**, *1971*, 903–995. [[CrossRef](#)]
30. Wu, Z.; Huang, N.E. A study of the characteristics of white noise using the empirical mode decomposition method. *Proc. R. Soc. Lond. A Math. Phys. Eng. Sci.* **2004**, *2046*, 1597–1611. [[CrossRef](#)]
31. Chowdhury, R.H.; Reaz, M.; Ali, M. Determination of muscle fatigue in SEMG signal using empirical mode decomposition. In Proceedings of the 2014 IEEE Conference on Biomedical Engineering and Sciences (IECBES), Kuala Lumpur, Malaysia, 8–10 December 2014; pp. 932–937.
32. Eliasson, A.-C.; Kruminde-Sundholm, L.; Rösblad, B.; Beckung, E.; Arner, M.; Öhrvall, A.-M.; Rosenbaum, P. The Manual Ability Classification System (MACS) for children with cerebral palsy: Scale development and evidence of validity and reliability. *Dev. Med. Child Neurol.* **2006**, *48*, 549–554. [[CrossRef](#)] [[PubMed](#)]
33. Andrade, A.O.; Nasuto, S.; Kyberd, P.; Sweeney-Reed, C.M.; Kanijn, F.R.V. EMG signal filtering based on Empirical Mode Decomposition. *Biomed. Signal Process. Control* **2006**, *1*, 44–55. [[CrossRef](#)]
34. Shabani, S.; Parsaei, H.; Shaabany, A. Classification of EMG Signals Using Empirical Mode Decomposition. *Int. J. Comput. Appl.* **2012**, *56*, 23–28.
35. Ramanand, P.; Nampoore, V.; Sreenivasan, R. Complexity quantification of dense array EEG using sample entropy analysis. *J. Integr. Neurosci.* **2004**, *3*, 343–358. [[CrossRef](#)] [[PubMed](#)]
36. Kamavuako, E.N.; Farina, D.; Jensen, W. Use of Sample Entropy Extracted from Intramuscular EMG Signals for the Estimation of Force. *Food Funct.* **2015**, *7*, 125–128.
37. Costa, M.; Healey, J.A. Multiscale entropy analysis of complex heart rate dynamics: Discrimination of age and heart failure effects. *Comput. Cardiol.* **2003**, *2003*, 705–708.
38. Flandrin, P.; Rilling, G.; Goncalves, P. Empirical mode decomposition as a filter bank. *Signal Process. IEEE Lett.* **2004**, *11*, 112–114. [[CrossRef](#)]
39. Arendt-Nielsen, L.; Mills, K.R.; Forster, A. Changes in muscle fiber conduction velocity, mean power frequency, and mean EMG voltage during prolonged submaximal contractions. *Muscle Nerve* **1989**, *12*, 493–497. [[CrossRef](#)] [[PubMed](#)]
40. Bigland-Ritchie, B.; Donovan, E.; Roussos, C. Conduction velocity and EMG power spectrum changes in fatigue of sustained maximal efforts. *J. Appl. Physiol.* **1981**, *51*, 1300–1305. [[PubMed](#)]
41. Pattichis, C.S.; Elia, A.G. Autoregressive and cepstral analyses of motor unit action potentials. *Med. Eng. Phys.* **1999**, *21*, 405–419. [[CrossRef](#)]
42. Boonstra, T.; Daffertshofer, A.; Van Ditschuijzen, J.; Van den Heuvel, M.; Hofman, C.; Willigenburg, N.; Beek, P. Fatigue-related changes in motor-unit synchronization of quadriceps muscles within and across legs. *J. Electromyogr. Kinesiol.* **2008**, *18*, 717–731. [[CrossRef](#)] [[PubMed](#)]
43. Holtermann, A.; Grönlund, C.; Karlsson, J.S.; Roeleveld, K. Motor unit synchronization during fatigue: Described with a novel sEMG method based on large motor unit samples. *J. Electromyogr. Kinesiol.* **2009**, *19*, 232–241. [[CrossRef](#)] [[PubMed](#)]
44. Moritani, T.; Muro, M.; Nagata, A. Intramuscular and surface electromyogram changes during muscle fatigue. *J. Appl. Physiol.* **1986**, *60*, 1179–1185. [[PubMed](#)]
45. Potvin, J.; Bent, L. A validation of techniques using surface EMG signals from dynamic contractions to quantify muscle fatigue during repetitive tasks. *J. Electromyogr. Kinesiol.* **1997**, *7*, 131–139. [[CrossRef](#)]
46. Naeije, M.; Zorn, H. Relation between EMG power spectrum shifts and muscle fibre action potential conduction velocity changes during local muscular fatigue in man. *Eur. J. Appl. Physiol. Occup. Physiol.* **1982**, *50*, 23–33. [[CrossRef](#)]
47. Sadoyama, T.; Masuda, T.; Miyano, H. Relationships between muscle fibre conduction velocity and frequency parameters of surface EMG during sustained contraction. *Eur. J. Appl. Physiol. Occup. Physiol.* **1983**, *51*, 247–256. [[CrossRef](#)]
48. Zwarts, M.; Van Weerden, T.; Haenen, H. Relationship between average muscle fibre conduction velocity and EMG power spectra during isometric contraction, recovery and applied ischemia. *Eur. J. Appl. Physiol. Occup. Physiol.* **1987**, *56*, 212–216. [[CrossRef](#)] [[PubMed](#)]

49. Castle, M.; Reyman, T.A.; Schneider, M. Pathology of spastic muscle in cerebral palsy. *Clin. Orthop. Relat. Res.* **1979**, *142*, 223–233. [[CrossRef](#)] [[PubMed](#)]
50. Ito, J.-I.; Araki, A.; Tanaka, H.; Tasaki, T.; Cho, K.; Yamazaki, R. Muscle histopathology in spastic cerebral palsy. *Brain Dev.* **1996**, *18*, 299–303. [[CrossRef](#)]
51. Milner-Brown, H.; Penn, R.D. Pathophysiological mechanisms in cerebral palsy. *J. Neurol. Neurosurg. Psychiatry* **1979**, *42*, 606–618. [[CrossRef](#)] [[PubMed](#)]
52. Rose, J.; Haskell, W.L.; Gamble, J.G.; Hamilton, R.L.; Brown, D.A.; Rinsky, L. Muscle pathology and clinical measures of disability in children with cerebral palsy. *J. Orthop. Res.* **1994**, *12*, 758–768. [[CrossRef](#)] [[PubMed](#)]
53. Rose, J.; McGill, K.C. Neuromuscular activation and motor-unit firing characteristics in cerebral palsy. *Dev. Med. Child Neurol.* **2005**, *47*, 329–336. [[CrossRef](#)] [[PubMed](#)]
54. Datta, A.; Farmer, S.; Stephens, J. Central nervous pathways underlying synchronization of human motor unit firing studied during voluntary contractions. *J. Physiol.* **1991**, *432*, 401–425. [[CrossRef](#)] [[PubMed](#)]
55. Farmer, S.; Swash, M.; Ingram, D.; Stephens, J. Changes in motor unit synchronization following central nervous lesions in man. *J. Physiol.* **1993**, *463*, 83–105. [[CrossRef](#)] [[PubMed](#)]
56. Kukulka, C.G.; Clamann, H.P. Comparison of the recruitment and discharge properties of motor units in human brachial biceps and adductor pollicis during isometric contractions. *Brain Res.* **1981**, *219*, 45–55. [[CrossRef](#)]



© 2016 by the authors; licensee MDPI, Basel, Switzerland. This article is an open access article distributed under the terms and conditions of the Creative Commons Attribution (CC-BY) license (<http://creativecommons.org/licenses/by/4.0/>).